On the Role of Grain Boundary Serration in Simulated Weld Heat-Affected Zone Liquation of a Wrought Nickel-Based Superalloy

HYUN UK HONG, IN SOO KIM, BAIG GYU CHOI, YOUNG SOO YOO, and CHANG YONG JO

The effects of grain boundary serration on boron segregation and liquation cracking behavior in a simulated weld heat-affected zone (HAZ) of a wrought nickel-based superalloy 263 have been investigated. The serrated grain boundaries formed by the developed heat treatment were highly resistant to boron segregation; the serrated sample contained 41.6 pct grain boundaries resistant to boron enrichment as compared with 14.6 pct in the unserrated sample. During weld thermal cycle simulation, liquated grain boundaries enriched with boron were observed at the peak temperature higher than 1333 K (1060 °C) in both unserrated and serrated samples; however, serrated grain boundaries exhibited a higher resistance to liquation. The primary cause of liquation in this alloy was associated with the segregation of the melting point depressing element boron at grain boundaries. The hot ductility testing result indicated that the serrated grain boundaries showed a lower susceptibility to liquation cracking; the grain boundary serration led to an approximate 15 K decrease in the brittle temperature range. These results reflect closely a significant decrease in interfacial energy as well as a grain boundary configuration change by the serration.

DOI: 10.1007/s11661-011-0837-2

I. INTRODUCTION

INTERGRANULAR microfissuring, which is frequently observed in a weld heat-affected zone (HAZ), is a main weldability concern in repair of nickel-based superalloys. It has been generally known that this microfissuring in HAZ is associated with constitutional liquation of precipitates at grain boundaries (GBs),[1–4] or incipient melting of GBs that are sufficiently segregated by melting point depressants, especially boron.[5,6] As HAZ liquation microfissuring is an intergranular phenomenon at elevated temperatures, the great concerns could be given to the character of GBs in the HAZ of superalloys.[5,7,8] For instance, Guo *et al.*[5] showed that the crystallographic character of GB influenced boron segregation, hence, GB liquation in the HAZ of Inconel 718 (Special Metals Corporation, New Hartford, NY). Therefore, grain boundary engineering (GBE) aims to increase the fraction of special boundaries that could be applied to superalloys to improve weldability as well as resistances to intergranular fracture caused by creep, fatigue, and stress-corrosion cracking. However, it has been realized that GBE processing,[9,10] which is achieved by repeated cycles of deformation and annealing, finds it difficult to be practically used in a wide range of applications.

It has been reported that GB serration can occur in nickel-based superalloys when controlled cooling treatments are employed.[11–15] The phenomenon of GB serration can be defined as the formation of serrated GB, which shows wavy morphology in nature. The serrated GBs are distinguishable from flat or smoothly-curved GBs because their amplitudes are larger than 500 nm.[15] Recently, the present authors have found that GB serration occurs in the absence of adjacent coarse γ' particles or $M_{23}C_6$ carbides when a specimen is direct-aged with a combination of slow cooling from solution treatment temperature to aging temperature.[16,17] They have shown that this serration leads to a change in GB character as a special boundary based on the crystallographic analysis, demonstrating that the GBs tend to serrate to have specific segments approaching to one {111} low-index plane at a boundary. They also found that the creep resistance can be improved up to 40 pct by GB serration in Alloy 263. The mechanisms of the formation and growth of GB serration are not clearly understood yet. However, they suggest that the driving force of serration stems from a sufficient decrease in interfacial free energy of GB even though the GB area is increased. This process would surely be accompanied by the decrease of the system's free energy.

The present work was initiated to study the possibility of GB serration as a viable means of improving the resistance of nickel-based superalloys to HAZ liquation cracking through an investigation on the influence of serration on boron segregation and liquation behavior.

HYUN UK HONG, Senior Researcher, IN SOO KIM, BAIG GYU CHOI, YOUNG SOO YOO, and CHANG YONG JO, Principal Researchers, are with the High Temperature Materials Research Group, Korea Institute of Materials Science, 797 Changwondaero, Sungsan-gu, Changwon, Gyeongnam 641-831, Republic of Korea. Contact e-mail: hnk@kims.re.kr
Manuscript submitted March 18, 2011.
Article published online July 28, 2011

II. EXPERIMENTAL PROCEDURES

The starting material was a commercially available hot-rolled Alloy 263 with composition (wt pct) Ni-20Co-20Cr-6Mo-0.06C containing <30 ppm boron present as a trace solute impurity. This alloy is age-hardened by precipitation of the global gamma-prime (γ') with a volume fraction of around 10 pct in the γ matrix. Studies were conducted on conventionally heat-treated (unserrated) and specially heat-treated (serrated) Alloy 263. For heat treatment, test samples of about 7 × 10 × 10 mm in size were cut from a piece of the alloy. The sample was solution-annealed [1423 K (1150 °C)/75 minutes] followed by water-quenching (WQ). The aging treatment [1073 K (800 °C)/8 hours] was then conducted. This heat treatment characterized by a two-step process is conventionally used for the alloy. The serrated sample was prepared through the special heat treatment designed proprietarily by the present authors[16–18] to contain the serrated GBs with a proportion of greater than 80 pct. The sample was solution-annealed at 1423 K (1150 °C) for 30 minutes and slow-cooled to 1073 K (800 °C) at a cooling rate of 10 K/min, and then subsequently aged for 8 hours at the same temperature. The average grain diameters of the unserrated and serrated samples were 127 and 110 μm, respectively.

The segregation of boron at GBs in each sample was detected using secondary ion mass spectrometry (SIMS). The SIMS analysis was performed in a Cameca Nano-SIMS 50 instrument (Cameca, Gennevilliers, France) using 16 keV Cs^+ as primary ions. SIMS ion images showing the distribution of boron in each sample were acquired by mass separating (mass resolution > 20,000) and imaging $^{11}B^{16}O^-$ molecular ions with atomic mass 27. The HAZ microstructures were simulated by a thermal cycle simulation system of Formastor FII (Fuji Electronic Industrial Co., Tokyo, Japan) equipped with a high-frequency induction specified by 400-kHz frequency/1.5-kW output. Cylindrical specimens of 3 mm diameter and 10 mm length were rapidly heated to 1173 K–1573 K (900 °C–1300 °C) at a rate of 111 K/s and then held for 1 second at each of the temperatures followed by helium gas quenching. The susceptibility of the alloy to HAZ cracking was evaluated by Gleeble hot ductility testing in a Gleeble 3500 (Dynamic Systems Inc., Poestenkill, NY) using a cylindrical specimen of 6 mm diameter and 110 mm length. The hot ductility testing was conducted in an argon atmosphere using a heating rate of 111 K/s, hold time at test temperature for 0.5 s, cooling rate of 19 K/s (for on-cooling tests), and a stroke rate of 25 mm/s. Scanning electron microscopy (SEM) was performed on a JEOL JSM-5800 microscope (Jeol, Tokyo, Japan) with a tungsten filament operating at 20 keV. The transmission electron microscopy (TEM) characterization was performed on a field emission type JEOL JEM-2100F (Jeol, Tokyo, Japan) operating at 200 keV.

III. RESULTS AND DISCUSSION

A. *The Formation of Serrated GBs by the Special Heat Treatment*

Figure 1 shows a comparison of microstructures depending on the occurrence of GB serration. The unserrated sample shows fine granular carbides distributed densely at flat GBs (Figure 1(a)). The GB carbides

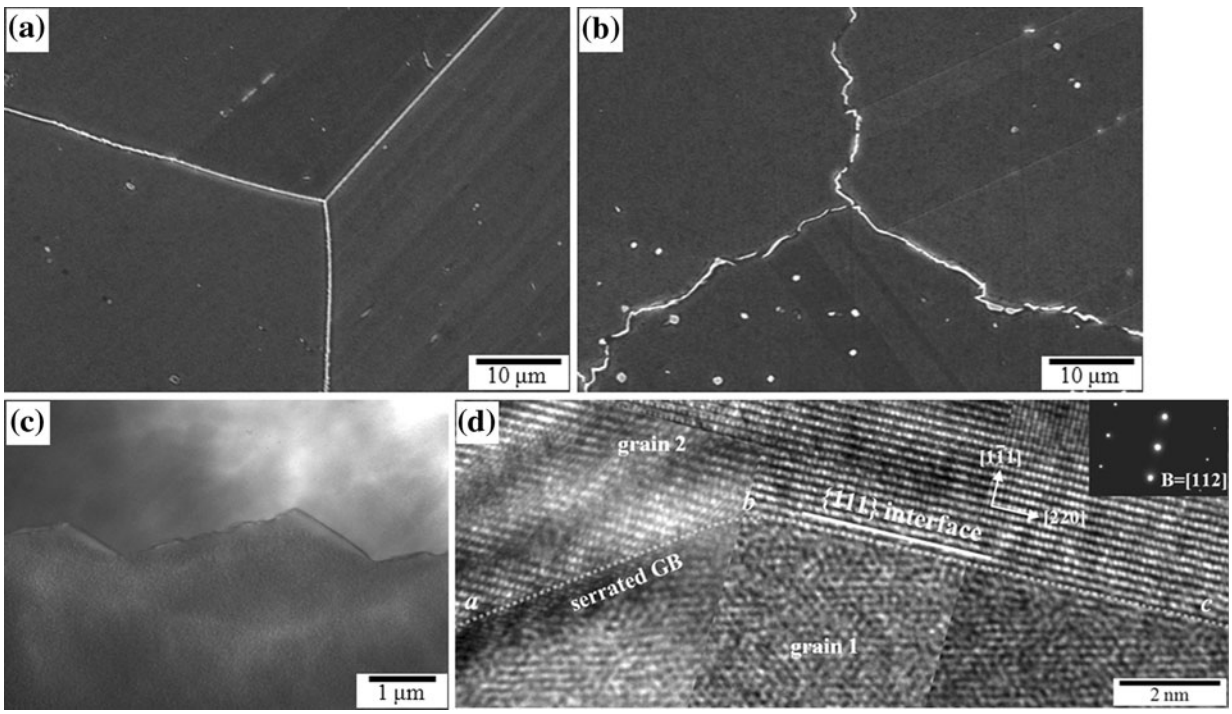

Fig. 1—Comparisons of GB morphology and carbide characteristics between (*a*) unserrated and (*b*) serrated samples. A typical serrated GB at the early stage of the slow cooling process: (*c*) TEM micrograph and (*d*) HR-lattice image (Beam direction = $[112]_{grain\ 2}$).

were identified as $M_{23}C_6$ with a very small fraction of MC, which is consistent with an earlier work done by Zhao *et al.*[19] On the other hand, the special heat treatment method characterized by a single step led successfully to GB serration. The serrated sample, in which GBs greater than 85 pct proportion are significantly serrated, contains planar carbides apart from each other at the serrated GBs (Figure 1(b)). At the early stage of the slow cooling process [when a specimen was cooled from 1423 K to 1273 K (1150 °C to 1000 °C) at 10 K/min], the GB began to be wavy, forming the serrated configuration. Figures 1(c) and (d) show that the typical serrated GBs appear prior to $M_{23}C_6$ precipitation. Neither carbide nor γ' particle could be observed on the serrated GB. Therefore, it is suggested that the GB serration occurs in the absence of $M_{23}C_6$ or the γ' particle, which is different from previous results of nickel-based superalloys claiming that the GB serrations are associated with the precipitation of adjacent coarse γ' particles or Ni_3Nb needles at the GBs.[11–15] It should be noted in Figure 1(d) that after the serration, the grain 2 plane terminates on the {111} low-index plane to make the "bc" wavy boundary segment. According to recent research,[20,21] the special boundaries with lower energy have been newly defined as those terminated by low-index boundary planes such as {111}. Thus, it might be inferred that the serrated GB is more preferable than flat GB in the viewpoint of interfacial free energy, which is responsible for the driving force of GB serration.

B. *Influence of the GB Serration on Boron Enrichment*

Comparing all the SIMS boron images with SEM micrographs of the same area allowed for measuring the boron-enriched GB fraction in each sample. The boron-enriched GB fraction is defined as the ratio of sum of boron-enriched GB length to total length of GB investigated. The SIMS boron images were obtained for approximately more than 150 GBs per specimen, and then image analysis was carried out. GBs were classified as resistant to boron enrichment if intensity was lower than 10^3 counts per second in the SIMS boron images. As shown in Figure 2, it is evident that the serrated GBs exhibit a higher resistance to boron enrichment than the unserrated GBs; the serrated sample contains 41.6 pct GBs resistant to boron enrichment as compared with 14.6 pct in the unserrated sample. Furthermore, comparison of the line scan profile across each GB revealed that the serrated GB shows smaller width of boron-enriched area as well as lower intensity (Figure 3). The boron-enriched GBs in both samples result from not only segregation of boron atoms to GBs but also incorporation of boron atoms into GB carbides. No appreciable segregation is found in the solutionized sample in which no GB carbides are present (intensity lower than 10^3 counts/sec). This result indicates that neither equilibrium segregation [held at 1423 K (1150 °C) for 75 minutes] nor nonequilibrium segregation associated with WQ (~500 K/s) is noticeable in the present study. Meanwhile, boron atoms segregate

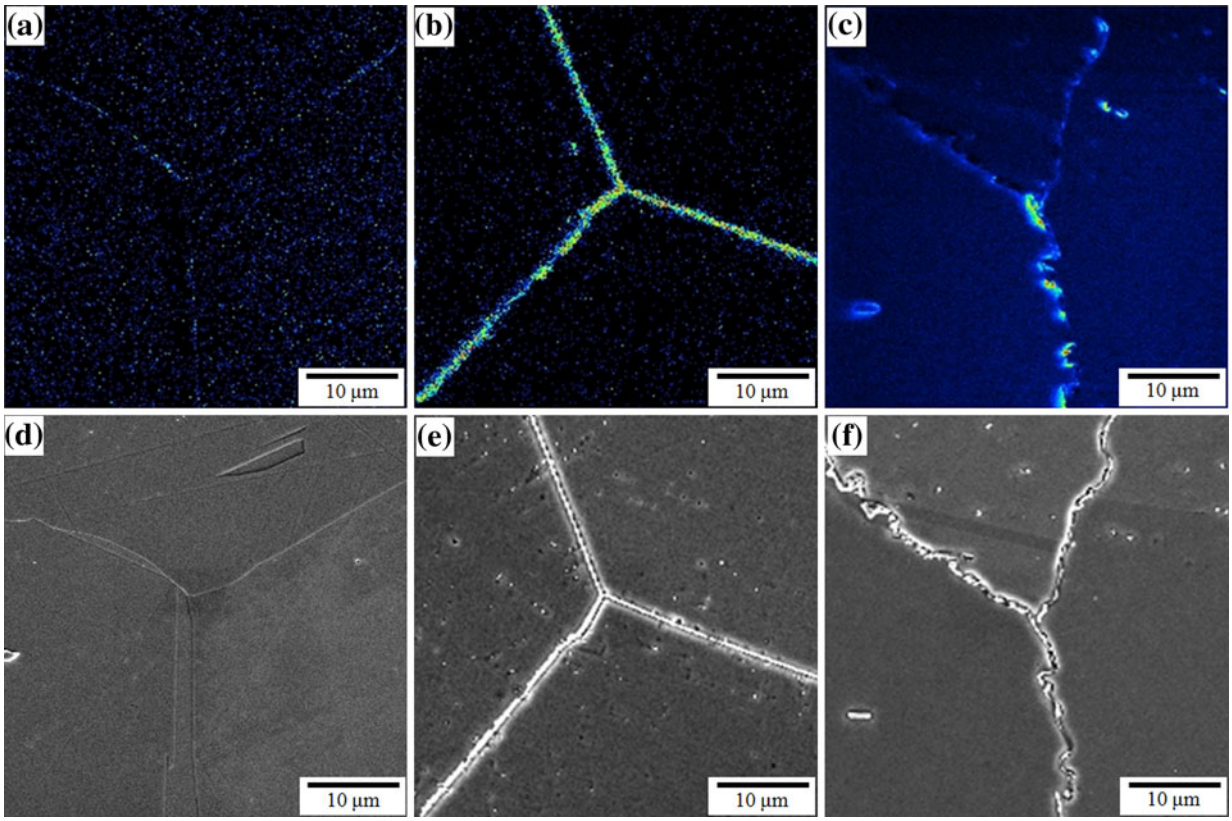

Fig. 2—SIMS boron images and corresponding SEM micrographs: (*a*), (*d*) for the solutionized sample, (*b*), (*e*) for the unserrated sample, and (*c*), (*f*) for the serrated sample.

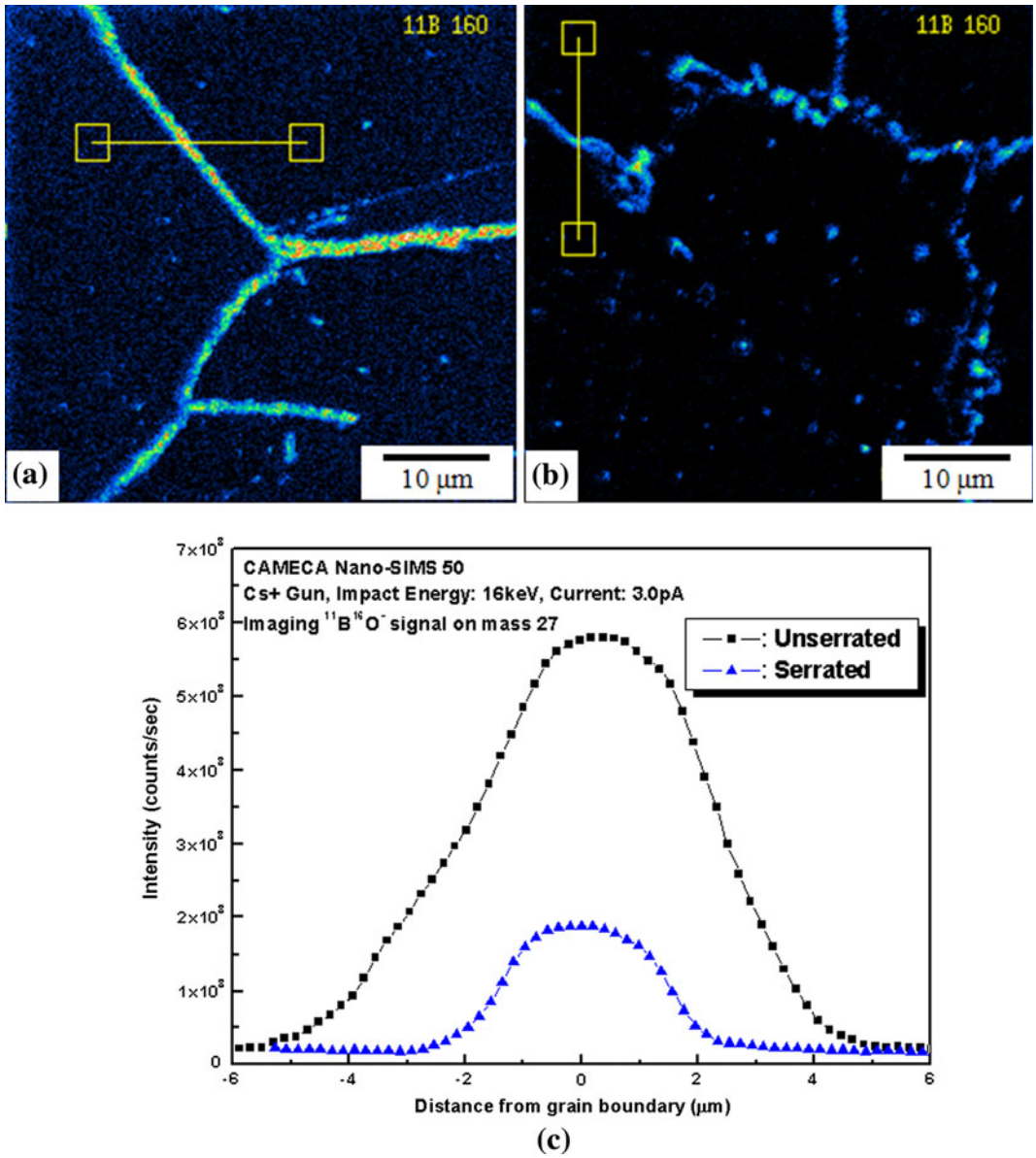

Fig. 3—SIMS boron images of (*a*) unserrated GB and (*b*) serrated GB and (*c*) line scan profile for each GB. The scanned line is indicated in each image shown in (a) and (b).

significantly to GBs during againg treatment because of their low solubility in nickel; then later most boron atoms become incorporated into GB carbides ($M_{23}C_6$ enriched with boron atoms). This result is consistent with earlier works[4,22–24] showing that the segregation-induced precipitation of boron containing paricles occurred during aging treatment at intermediate temperatures [1023 K to 1323 K (750 °C to 1050 °C)].

It has been well known that boron atoms segregate to GBs by equilibrium and nonequilibrium segregation.[25–27] Thus, the different heat treatment may affect the boron segregation behavior. The main difference in heat treatment for the formation of serrated GBs was the existence of slow cooling (10 K/minute) from solution temperature to aging temperature. Karlsson *et al.*[26,27] showed that in austenitic stainless steel 316L, the boron segregation behavior was mainly of the nonequilibrium type, and a larger amount was observed when the specimen was cooled slower than WQ. This result can be understood by a model based on mobile vacancy-boron atom pairs diffusing down vacancy gradients toward vacancy sinks (*i.e.,* GB, interface) during cooling.[26,27] The degree of segregation becomes higher if the cooling rate is lower than WQ because the time becomes sufficient to let vacancy-boron atom pairs diffuse to the GB.[28] Therefore, it can be inferred that the heat treatment for GB serration, associated with slow cooling, should be more susceptible to large boron segregation by nonequilibrium type than conventional heat treatment. Nevertheless, the serrated GBs are highly resistant to boron enrichment compared with the unserrated GBs (Figures 2 and 3). This large difference

in boron enrichment at GBs between the unserrated and serrated samples can be attributed to the different GB characters. For nonequilibrium segregation, the important factor is the ability of the boundary to act as a vacancy sink. Special GBs are not available while random GBs (loosely packed GB interfaces) can operate as highly efficient vacancy sinks.[29] Thus, the serrated GBs being considered as special boundaries may be resistant to nonequilibrium boron segregation. For equilibrium segregation (during isothermal aging treatment), significant variations in boron concentrations of each GB are related with GB character.[5,26,27,30] According to McLean,[25] the equilibrium concentration of segregating atoms at GBs can be expressed by:

$$C_b = C_m \cdot \exp(E_b/kT)/(1 + C_m \cdot \exp(E_b/kT)) \quad [1]$$

where C_m is the concentration of solute atoms in the matrix, k is Boltzman's constant, T is temperature, and E_b is the binding energy between the segregant and GB. It can be seen that GB segregation would depend largely on this binding energy (E_b), which is governed by the nature of the segregating element and the interfacial energy of GBs.[5,27] Hence, the interfacial energy of GB would determine the degree of boron segregation during aging treatment because the same boron content and negligible grain size difference between the unserrated and serrated samples are considered in the present study. As a similar way in the nonequilibrium segregation, the serrated GBs with lower interfacial energy may be resistant to equilibrium boron segregation while boron atoms are more likely to segregate into the unserrated GBs. Similarily, Kurban *et al.*[30] showed that GB-engineered alloy 304 displayed a higher resistance to intergranular boron segregation than conventionally processed alloy 304 because of its higher frequencies of low Σ boundaries.

C. *Influence of the GB Serration on Liquation Cracking Behavior During Weld Thermal Cycle Simulation*

Observation of the simulated HAZ microstructures has been carried out to understand the microstructural response in the weld HAZ of the alloy. At a peak temperature higher than 1333 K (1060 °C), GB carbides were no longer observed in both samples, as previously observed.[31] Instead, liquated GBs enriched with boron were observed in the present study. One example of simulated HAZ microstructure variation with peak temperatures is shown for the unserrated sample (Figure 4). Because of rapid heating simulated by the weld thermal cycle, the $M_{23}C_6$ carbide remains even to temperatures well above its equilibrium solvus temperature [1208 K (935 °C)]. Instead of the carbide dissolution, it is probable that this GB carbide could constitutionally liquate by eutectic-type reaction with the surrounding γ matrix at the temperature higher than 1333 K (1060 °C). Constitutional liquation of second-phase particles during rapid heating of two-phase alloys was first proposed by Pepe and Savage.[1] The liquation phenomenon is known to occur generally by an eutectic-type reaction between a second-phase particle and the matrix producing a nonequilibrium solute-rich film at such a particle/matrix interface. The basic requirement for the occurrence of constitutional liquation of a second-phase intermetallic particle in an alloy is the existence of such a particle at a temperature equal to or above the eutectic reaction temperature during heating. Therefore, the susceptibility of such an intermetallic particle to constitutional liquation is dependent on its solid-state dissolution behavior during rapid heating.[4] However, Owczarski[32] insisted that $M_{23}C_6$ particles would undergo a solid-state reaction well below the solidus temperature and would not liquate during

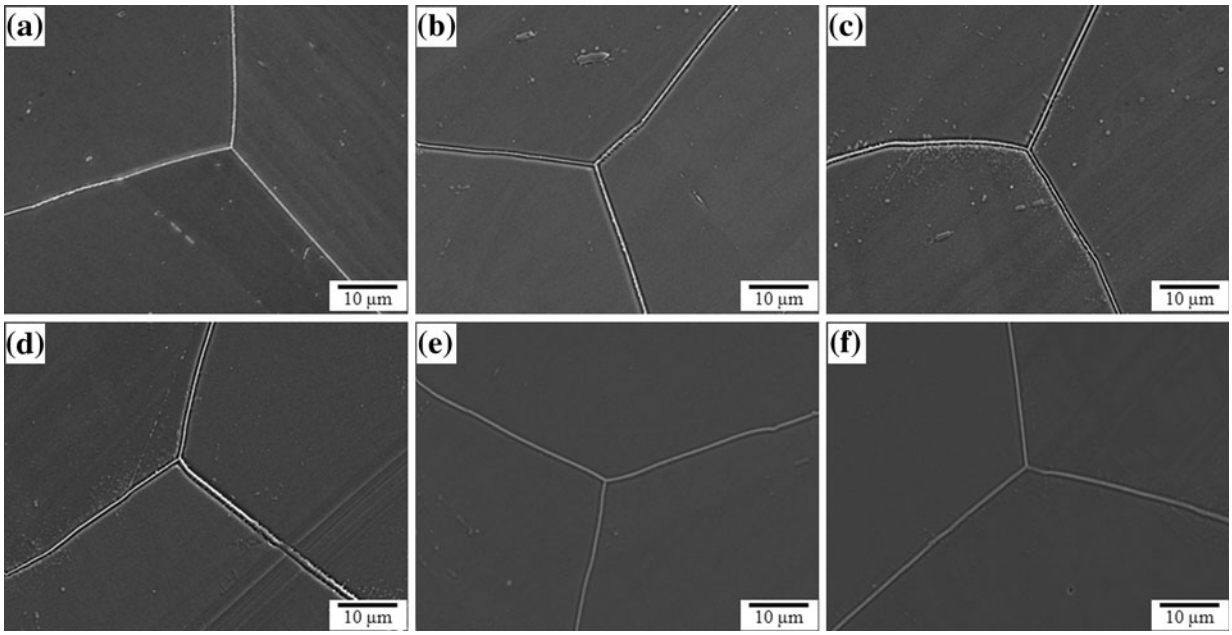

Fig. 4—Simulated HAZ microstructure variation with peak temperatures (T_p): (*a*) before simulation, (*b*) T_p = 1223 K (950 °C), (*c*) T_p = 1273 K (1000 °C), (*d*) T_p = 1313 K (1040 °C), (*e*) T_p = 1333 K (1060 °C), and (*f*) T_p = 1353 K (1080 °C).

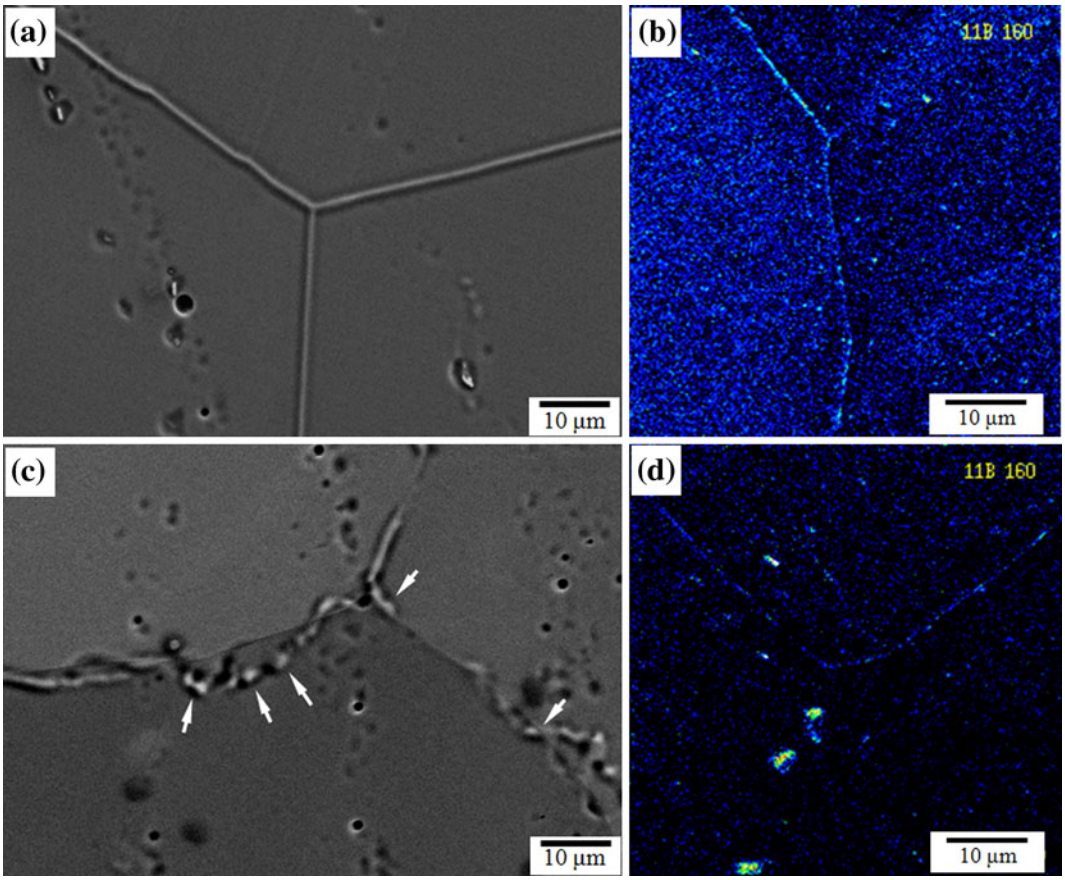

Fig. 5—HAZ microstructures and SIMS boron images in samples simulated at 1453 K (1180 °C): (*a*), (*b*) for the unserrated sample and (*c*), (*d*) for the serrated sample. The arrows indicate the liquid pocket in Fig. 5(c).

welding. In the present study, the liquated regions on GBs show a similar composition with the matrix except higher boron content in both samples (Figure 5). No other atoms such as Cr, P, S, Mo, and Ti were detectable at the liquated GB regions within the limitation of the TEM/EDS system. This result implies that the cause of GB liquation in Alloy 263 is not predominantly associated with the constitutional liquation of $M_{23}C_6$ precipitates. The melting point depressing element boron could be primarily involved in the liquation because its segregation at GBs significantly lowers the melting point of the boundaries.[4–6,22–24,28] Thus, the GB liquation in both samples simulated at and above 1333 K (1060 °C) seems to be related to boron enrichment during aging treatment. GBs may be infiltrated by a liquid layer considerably below the bulk melting temperature if wetting occurs.

The GB liquation behavior is closely related with the GB character. HAZ microstructures simulated at 1453 K (1180 °C) were observed, an example of which is shown in Figure 5. Liquated GBs are more prominent in the unserrated specimen rather than in the serrated one. Even the liquated segments are observed apart from each other at the GBs, and GB carbides remain occasionally in the serrated specimen. If the liquated GB fraction is defined as the ratio of the sum of liquated GB length to total length of GB investigated, the serrated specimen shows 77.5 pct, whereas the unserrated one shows 93.9 pct (based on examination of 150 ~ 200 GBs). As previously discussed, flat GBs in Alloy 263 are more likely to be of a "random" nature with interfacial planes far from low-index planes rather than from serrated GBs.[16–18,31] Random flat GBs are inherently of higher energy than the serrated GBs considered as "special boundaries." This difference in a character of GB could be responsible for different wettability of GB liquid film from each other besides different boron enrichment. The distribution of intergranular liquid could be considered along with a GB wetting relationship proposed by Smith[33]:

$$\gamma_{gb} = 2\gamma_{sl}\cos\theta \qquad [2]$$

where θ is the wetting angle, γ_{gb} is the GB energy, and γ_{sl} is the solid–liquid interface energy. It is evident from Eq. [2] that for a given solid–liquid interfacial energy, the higher the GB energy, the higher the tendency for GB to be wetted and penetrated by the liquid phase.[4] The difference in a character of GB could be a factor in aiding extensive GB wetting and penetration by liquid film in Alloy 263. As observed in the present work (Figure 5(c)), the liquid will exist in isolated pockets allowing substantial intergranular solid–solid contact if wetting is ineffective as a result of a lower GB energy (a higher wetting angle as seen from Eq. [2]). On the other hand, the flat GBs in the unserrated specimen are

Table I. Gleeble Hot Ductility Test Results for Both Unserrated and Serrated Samples

Material	NDT [K (°C)]	NST [K (°C)]	DRT [K (°C)]	T_p [K (°C)]	ZDTR [K (°C)]	LTR [K (°C)]	T_L [K (°C)]
Unserrated	1528 (1255)	1584 (1311)	1523 (1250)	1553 (1280)	105 (105)	61 (61)	1633 (1360)
Serrated	1543 (1270)	1577 (1304)	1528 (1255)	1553 (1280)	90 (90)	49 (49)	1633 (1360)

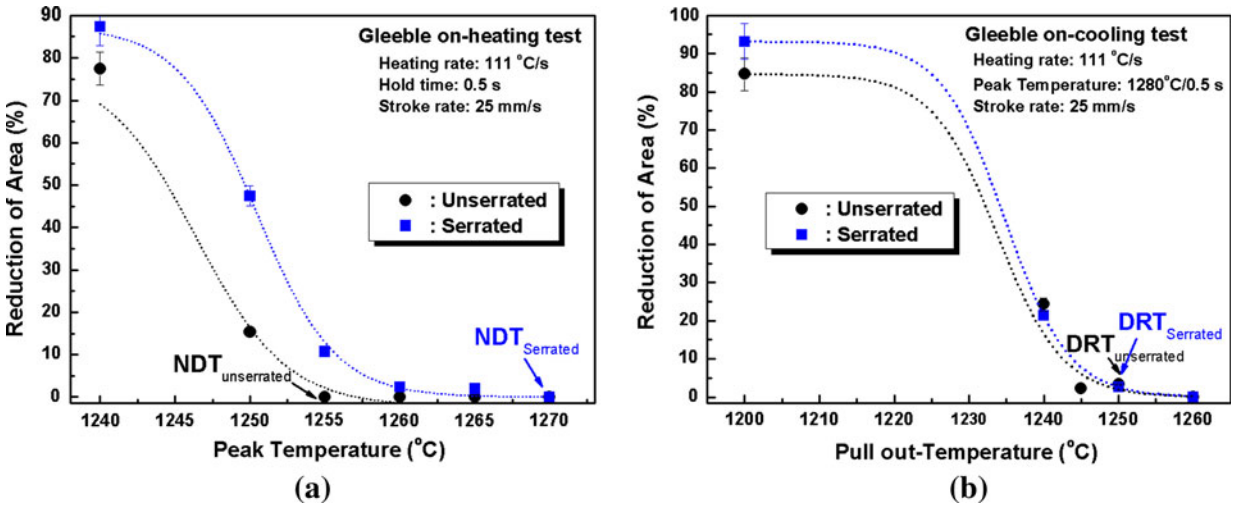

Fig. 6—Relationships between ductility and temperature at which tensile loading is applied: (*a*) on-heating tests for nil ductility temperature (NDT) and (*b*) on-cooling tests for ductility recovery temperature (DRT).

observed to be liquated in a continuous fashion (Figure 5(a)). This higher wettability could be partly attributed to a character of flat GBs with a random nature (a higher GB interfacial energy) even though carbide characteristics such as density, size, and morphology may also affect GB wetting behavior. The present investigation is consistent with the correlation established in earlier studies[5,6,8] showing that liquid penetration at the GB was greatest at high-angle boundaries and was relatively insignificant at low-angle boundaries. Thus, it can be suggested that the higher resistance of the serrated GB to liquation is most likely to be related with its lower GB energy, causing them less boron enrichment and lower wettability as compared with the random flat GBs. These combined effects of the serrated GB would make it more difficult to cause HAZ liquation cracking.

Gleeble hot ductility results for both the unserrated and the serrated samples are given in Table I.

This test is based on the premise that the deformation behavior of a material, as evaluated by its hot ductility, reflects its capability to accommodate tensile stresses and resist cracking during the welding thermal cycle.[4] The critical hot ductility data were obtained to quantify the weldability in terms of nil ductility temperature (NDT), nil strength temperature (NST), ductility recovery temperature (DRT), the zero ductility temperature range (ZDTR) between the liquidus temperature (T_L) and NDT, and the liquation temperature range (LTR) between DRT and NST for the on-cooling test. Within the ZDTR (on-heating) and the LTR (on-cooling), the materials show no ductility. Therefore, the ZDTR and LTR value can be used to quantify susceptibility to liquation cracking, with larger values indicating higher susceptibility. The NDT and DRT were determined based on the ductilty-temperature relationship as shown in Figure 6. The Gleeble hot ductility results indicate that the serrated sample shows a lower susceptibility to liquation cracking than the unserrated one; the GB serration leads to an approximate 15 K decrease in the brittle temperature range where HAZ liquation cracking is most likely to occur. As shown in Figure 7, the serrated samples show frequently wavy features on the intergranular fractured surface, whereas sharp GB facets associated with little plastic deformation can be seen in the unserrated sample. These local ductile regions in the serrated sample imply a significant resistance to intergranular liquation crack propagation.

IV. CONCLUSIONS

The results of the present study indicate that the GB serration influences the behavior of intergranular HAZ liquation cracking of a wrought nickel-based superalloy through the modification of GB characters. The serrated GBs exhibit a lower susceptibility to HAZ liquation cracking as a result of the combined effect of boron segregation and wettability; the serrated GBs are highly resistant to boron segregation, and they show a lower HAZ liquation tendency during thermal cycle simulation. These results reflect closely a significant decrease in interfacial energy as well as GB configuration change by the serration. The present work has

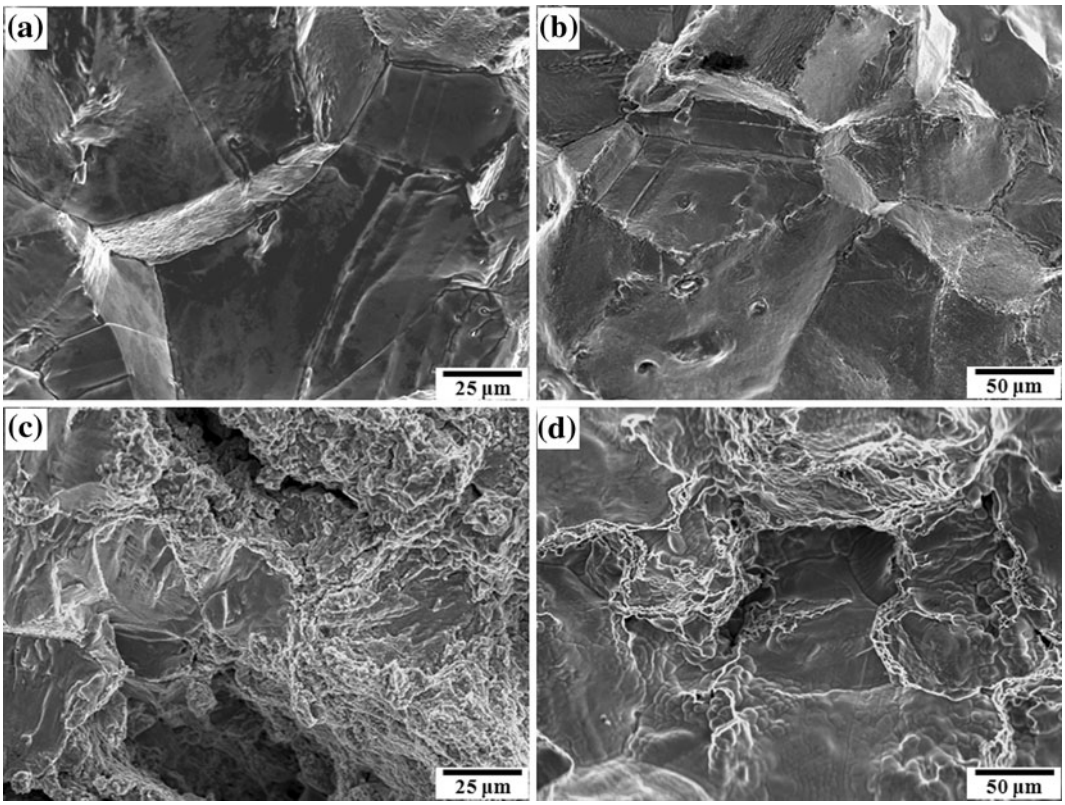

Fig. 7—Comparison of fractured surfaces after hot ductility test at 1523 K (1250 °C): On-heating test for (*a*) the unserrated sample and (*c*) the serrated sample, and on-cooling test for (*b*) the unserrated sample and (*d*) the serrated sample.

found a possibility of GB serration as a viable means of improving the resistance of nickel-based superalloys to HAZ liquation cracking as well as high temperature performance.

ACKNOWLEDGMENTS

The authors are grateful for the financial support from MKE (Ministry of Knowledge Economy), Account No. UCN215-2848.C and 615-2848.C, which made this work possible. The authors also would like to thank Dr. Hong at KBSI, Busan for his sincere assistance with the nano-SIMS analysis.

REFERENCES

1. J.J. Pepe and W.F. Savage: *Weld. J.*, 1967, vol. 46, pp. 411s–422s.
2. R. Nakkalil, N.L. Richards, and M.C. Chaturvedi: *Scripta Metall. Mater.*, 1992, vol. 26, pp. 1599–1604.
3. R. Vincent: *Acta Metall.*, 1985, vol. 33, pp. 1205–16.
4. O.A. Ojo and M.C. Chaturvedi: *Metall. Mater. Trans. A*, 2007, vol. 38A, pp. 356–69.
5. H. Guo, M.C. Chaturvedi, N.L. Richards, and G.S. McMahon: *Scripta Mater.*, 1999, vol. 40, pp. 383–88.
6. K.R. Vishwakarma, N.L. Richards, and M.C. Chaturvedi: *Mater. Sci. Eng. A*, 2008, vol. 480, pp. 517–28.
7. H. Kokawa, C.H. Lee, and T.H. North: *Metall. Trans. A*, 1991, vol. 22A, pp. 1627–31.
8. M. Qian and J.C. Lippold: *Acta Mater.*, 2003, vol. 51, pp. 3351–61.
9. P. Lin, G. Palumbo, U. Erb, and K.T. Aust: *Scripta Metall. Mater.*, 1995, vol. 33, pp. 1387–92.
10. N. Souaï, N. Bozzolo, L. Nazé, Y. Chastel, and R. Logé: *Scripta Mater.*, 2010, vol. 62, pp. 851–54.
11. J.M. Larson and S. Floreen: *Metall. Trans. A*, 1977, vol. 8A, pp. 51–55.
12. A.K. Koul and G.H. Gessinger: *Acta Metall.*, 1983, vol. 31, pp. 1061–69.
13. A.K. Koul and R. Thamburaj: *Metall. Trans. A*, 1985, vol. 16A, pp. 17–26.
14. A.K. Koul, P. Au, N. Bellinger, R. Thamburaj, W. Wallace, and J-P. Immarigeon: *Superalloys 1988*, Eds. S. Reichman, D.N. Duhl, G. Maurer, S. Antolovich, and C. Lund, TMS, Warrendale, PA, 1988, pp. 3–12.
15. H. Loyer Danflou, M. Marty, and A. Walder: *Superalloys 1992*, Eds. S.D. Antolovich, R.W. Stusrud, R.A. MacKay, D.L. Anton, T. Khan, R.D. Kissinger, and D.L. Klarstrom, TMS, Warrendale, PA, 1992, pp. 63–72.
16. H.U. Hong, I.S. Kim, B.G. Choi, M.Y. Kim, and C.Y. Jo: *Mater. Sci. Eng. A*, 2009, vol. 517, pp. 125–31.
17. H.U. Hong, H.W. Jeong, I.S. Kim, B.G. Choi, Y.S. Yoo, and C.Y. Jo: *Mater. Sci. Forum*, 2010, vols. 638–642, pp. 2245–50.
18. H.U. Hong, I.S. Kim, B.G. Choi, C.Y. Jo, Y.S. Yoo, H.W. Jeong, and S.M. Seo: US Patent Application Serial No. 12/484,597.
19. J.C. Zhao, V. Ravikumar, and A.M. Beltran: *Metall. Mater. Trans. A*, 2001, vol. 32A, pp. 1271–82.
20. V. Randle: *Scripta Mater.*, 2006, vol. 54, pp. 1011–15.
21. G.S. Rohrer, V. Randle, C.S. Kim, and Y. Hu: *Acta Mater.*, 2006, vol. 54, pp. 4489–4502.
22. B. Hu and H. Li: *Superalloys 1980*, Eds. J.K. Tien, S.T. Wlodek, H. Morrow III, M. Gell, and G.E. Maurer, TMS, Warrendale, PA, 1980, pp. 423–29.
23. R.M. Kruger and G.S. Was: *Metall. Trans. A*, 1988, vol. 19A, pp. 2555–66.

24. W. Chen, M.C. Chaturvedi, N.L. Richards, and G. McMahon: *Metall. Mater. Trans. A*, 1998, vol. 29A, pp. 1947–54.
25. D. McLean: *Grain Boundaries in Metals*, Clarendon Press, Oxford, UK, 1957.
26. L. Karlsson, H. Nordén, and H. Odelius: *Acta Metall.*, 1988, vol. 36, pp. 1–12.
27. L. Karlsson and H. Nordén: *Acta Metall.*, 1988, vol. 36, pp. 13–24.
28. W. Chen, M.C. Chaturvedi, and N.L. Richards: *Metall. Mater. Trans. A*, 2001, vol. 32A, pp. 931–39.
29. R.W. Balluffi: *Metall. Trans. A*, 1982, vol. 13A, pp. 2069–95.
30. M. Kurban, U. Erb, and K.T. Aust: *Scripta Mater.*, 2006, vol. 54, pp. 1053–58.
31. H.U. Hong, I.S. Kim, B.G. Choi, H.W. Jeong, S.M. Seo, Y.S. Yoo, and C.Y. Jo: *Mater. Sci. Forum*, 2010, vols. 654–656, pp. 488–91.
32. W.A. Owczarski: *Welding Research Council Bulletin*, New York, NY, 1969, pp. 6–9.
33. C.S. Smith: *Trans. AIME*, 1948, vol. 175, pp. 15–51.